The importance of polarizability in the modeling of ionic diffusion in ceria

IOP Conf. Series: Materials Science and Engineering **169** (2017) 012002 doi:10.1088/1757-899X/169/1/012002

The importance of polarizability in the modeling of ionic diffusion in ceria

A K Lucid[1], **G W Watson**[1]

[1]School of Chemistry and CRANN, Trinity College Dublin, College Green, Dublin 2, Ireland

E-mail: lucida@tcd.ie, watsong@tcd.ie

Abstract. Classical molecular dynamics can be used to investigate ionic diffusion and its limitations in trivalently doped ceria and at the surfaces and interfaces of these materials. Here we compare the performance of two interatomic potentials derived for samarium doped ceria from the same set of ab-initio data, a dipole polarizable ion model (DIPPIM) and a rigid ion model (RIM). The DIPPIM allows for polarization effects resulting from induced dipoles whereas the RIM does not. In this study we aim to elucidate whether or not this system can be modelled successfully using a RIM or if a DIPPIM is necessary due to the large polarization effects caused by the presence of oxide (O^{2-}) ions.

1. Introduction

Oxide ions, which are the charge carriers in oxide ion conducting materials, are highly polarizable which is often ignored when modeling these materials.[1, 2, 3] Polarizability can be accounted for in interatomic potentials in a number of ways; shell models[4], embedded atom models[5, 6] and models where dipoles are solved self consistently as a response to changes in electric field[7] can all be utilized. These polarizable models can be computationally expensive and very time consuming, particularly those which calculate dipoles self consistently, and so it is worthwhile to determine whether or not the polarizability of the oxide ions must be taken into account.

Solid oxide fuel cells (SOFCs) are an example of a device in which oxide ion conduction is essential to the performance of the system. These devices offer an alternative for efficient, clean and renewable energy conversion in this environmentally conscious era.[8] These devices currently require high temperatures ($\sim$1273K) to operate; this is necessary for oxide ion diffusion in the electrolyte to occur. The most commonly used electrolyte materials in these devices is yttria-stabilized zirconia(YSZ). These high temperatures contribute to the cost, performance degradation and inefficiency of current SOFCs. Ceria (CeO_2) doped with trivalent cations has been suggested as a material which could replace YSZ as the solid electrolyte as it can achieve ionic conductivities comparable to YSZ but in the intermediate temperature (IT) range of 773-1073K. [9] Samarium (Sm) and gadolinium (Gd) are the dopants which have been seen to perform best with ceria as SOFC electrolytes.[10, 11] In order to optimize these materials for applications (i.e. to understand behaviors at surfaces and interfaces) we need to have a model which can accurately calculate the conductivities and diffusion mechanisms in these systems.

Here we present a comparison of a rigid ion model (RIM) and a dipole polarizable ion model (DIPPIM)[7] which have both been fitted to the same set of ab initio data[12]; the RIM is $\sim$10 times less computationally demanding than the DIPPIM. However, the DIPPIM is orders

of magnitude less computationally expensive than ab initio MD; ab initio MD would not be tractable for the size of cells which we use to perform calculations. By fitting to ab initio potential energy surfaces, with accurate inclusion of polarizability, DIPPIM allows ab initio quality MD for a fraction of the cost. The testing was carried out on Sm-doped CeO_2 and pure CeO_2 by investigation of ionic conductivity, activation energy, structure, defect interactions and phonon modes.

2. The interatomic potentials

The RIM and DIPPIM interatomic potentials used here have been fitted to identical force, stress and dipole data which was generated using hybrid-DFT calculations.[12] They both include a pair potential, which is comprised of Coulombic interactions, a modified Buckingham type short-range repulsive term and a dispersion term, as described by Castiglione *et al.*[7] In the DIPPIM, polarization effects resulting from induced dipoles on ions in the system are taken into account. The part of the potential which is associated with the polarization includes only dipolar effects. The induced dipole on each ion for a given configuration is obtained by minimization, at each MD step, of the following potential with respect to all dipoles ($\boldsymbol{\mu}_i$):

$$U^{pol} = \sum_{j\neq i}^{N}[f_{ij}^{*}\mathbf{T}^{(1)}(\mathbf{r}_{ij})\cdot(q_j\boldsymbol{\mu}_i - q_i\boldsymbol{\mu}_j) + \sum_{j\neq i}^{N}\boldsymbol{\mu}_i\cdot\mathbf{T}^{(2)}(\mathbf{r}_{ij})\cdot\boldsymbol{\mu}_j] + \sum_{i=1}^{N}\frac{1}{2\alpha_i}|\boldsymbol{\mu}_i|^2 \quad (1)$$

$$f_{ij}^{*} = 1 - c_{ij}^{*}e^{-b_{ij}^{*}r_{ij}}\sum_{k=0}^{4}\frac{(b_{ij}^{*}r_{ij})^k}{k!} \quad (2)$$

Where q_i is the formal ionic charge on each ion, and the interaction tensors $\mathbf{T}^{(1)}(\mathbf{r}_{ij})$ and $\mathbf{T}^{(2)}(\mathbf{r}_{ij})$ are the charge-dipole and dipole-dipole interaction tensors. The first term in Equation 1 represents the charge-dipole interactions between atoms i and j. This interaction is damped by a Tang-Toennies function (f_{ij}^{*}, Equation 2), to account for short-range induction effects. The second term accounts for the dipole-dipole interactions and the final term is the potential energy of the polarization, where $\boldsymbol{\alpha}_i$ is the polarizability of the ion. This is the energy required to polarize the ion. It is the optimization of the dipole energy (Equation 1) which accounts for the computational expense of the DIPPIM.

3. Simulation details

Calculations were carried out using the finite temperature molecular dynamics program PIMAIM [13]. All simulations were carried out on 6×6×6 supercells of $Ce_{1-x}Sm_xO_{2-x/2}$ equating to ∼2592 atoms depending the the dopant concentration. Calculations were carried out at five dopant concentrations (x = 0.05, 0.10, 0.15, 0.20, and 0.25) and at three temperatures, spanning the IT range (773K, 973K, and 1173K). To account for the statistical nature of MD, three randomized configurations of dopants and oxygen vacancies were considered for each dopant concentration. As a result of running calculations on three configurations values such as ionic conductivity and activation energy can be reported as average values.

Each system was first optimized, and temperature scaling was then carried out every 0.025ps for 10ps. The supercells were allowed 40ps to come to thermal equilibrium before data collection for analysis began. The data collection runs were 3ns for 773K and 1ns for 973K and 1173K. An isothermal-isobaric ensemble (NPT)[14] was used, with a timestep of 4fs. The short-range cutoff for the interatomic potentials and the cutoff for the Ewald sum was 11Å.

4. Results and discussion

4.1. Ionic conductivity and activation energy

The diffusion coefficient, D, was calculated from the mean squared displacement (MSD) of the trajectory of the oxide ions and was used to calculate the ionic conductivity from the Nernst-Einstein equation:

$$\sigma = \left(\frac{\rho q^2}{H_R k_B T}\right) D \tag{3}$$

where ρ is the number density of the charge carriers (in this case these are the oxide ions), q is the effective charge of the charge carriers, H_R is the Haven ratio (=1), k_B is Boltzmann's constant and T is the temperature of the system. The ionic conductivity, at 973K, for both the RIM and the DIPPIM is displayed in Figure 1(a), and it can be seen that there is at least an order of magnitude difference between the two models. The ionic conductivities for the RIM and DIPPIM are compared to experiment in Figure 1(b), with the experimental studies by Zha *et al.* and Jung *et al.* [11, 15] selected to show the variation in the literature, both in ionic conductivity and in the concentration at which the maximum in conductivity is seen. It can quite clearly be seen from Figure 1 that the DIPPIM is significantly better than the RIM at calculating ionic conductivities comparable to experiment which is vital to the performance of these materials as solid electrolytes.

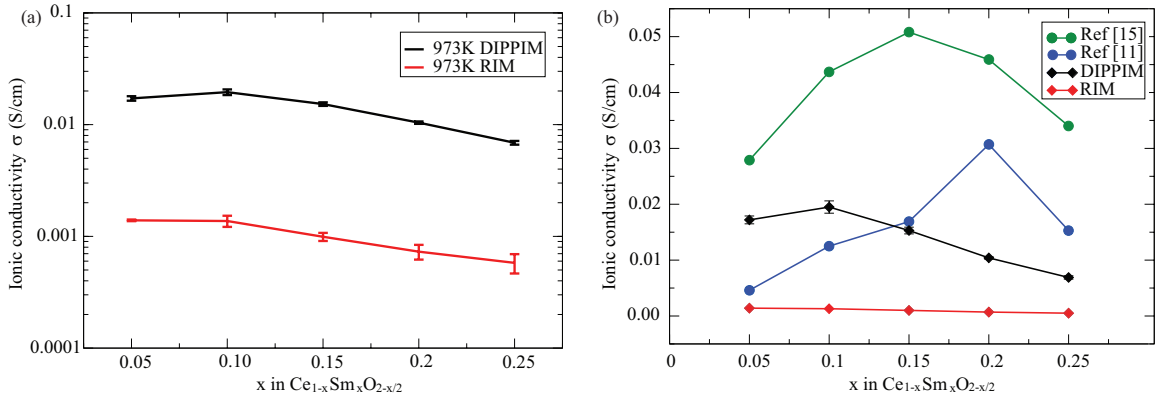

Figure 1. The ionic conductivity of $Ce_{1-x}Sm_xO_{2-x/2}$ at 973K for DIPPIM (black) and RIM (red) is shown in (a); it should be noted that this is a log scale. The ionic conductivity of the DIPPIM, RIM and two experimental studies[15, 11](green and blue) are shown at 973K in (b).

The activation energy for ionic conductivity can be calculated using:

$$\sigma T = \sigma_0 \exp\left(-\frac{E_a}{k_B T}\right) \tag{4}$$

where E_a is the activation energy, σ_0 is the attempt frequency of the hopping process, and all other terms are as previously defined. A plot of $\ln(\sigma T)$ versus $1/T$ was used to obtain the E_a of $Ce_{0.9}Sm_{0.1}O_{1.95}$ from 773K to 1173K (Table 1). Both the RIM and DIPPIM are in good agreement with experiment, suggesting that the activation energy of diffusion is being correctly described by both models. However, based on the results seen for ionic conductivity, it suggests that the RIM may not correctly model the attempt frequency of the hops.

Table 1. Activation energy for ionic conductivity of $Ce_{0.9}Sm_{0.1}O_{1.95}$ (E_a) for both the DIPPIM and RIM, compared to experiment.

E_a (eV)	Reference
0.610	DIPPIM
0.607	RIM
0.645	[11]
0.628	[16]
0.615	[17]

4.2. Structure

The partial radial distribution functions (RDFs) for Ce-O, Sm-O and O-O were all calculated; no major discrepancies were seen between the two models, with the RIM showing slightly sharper peaks which could be accounted for by the difference in dynamics between the RIM and DIPPIM. The dopant-vacancy (Sm-Vac) and vacancy-vacancy (Vac-Vac) RDFs were also calculated; these are shown for $Ce_{0.9}Sm_{0.1}O_{1.95}$ at 973K in Figure 2. The Ce-O and O-O RDFs are plotted with the Sm-Vac and Vac-Vac RDFs as these represent a random distribution of cations and vacancies when no ordering has occurred. On investigation of the Sm-Vac RDFs there is a very clear difference seen between the RIM and DIPPIM Sm-Vac distribution. For the RIM there is trapping of the vacancies in the nearest-neighbor site to the Sm ions. As the same is not seen for DIPPIM, it would appear that the RIM is severely overestimating the attraction between the dopant cations and vacancies which may be responsible for the severe drop in ionic conductivity that is seen when using the RIM. For the Vac-Vac RDF it can be seen that the DIPPIM predicts enhanced vacancy ordering in the $\langle 111 \rangle$ direction of the anion sub-lattice when compared with the RIM, although the long-range ordering is in agreement with the DIPPIM. This enhanced vacancy ordering in the $\langle 111 \rangle$ direction has been seen for doped fluorite materials previously and is believed to be the main reason for the drop in ionic conductivity of these materials past a certain vacancy concentration.[18, 19, 20]

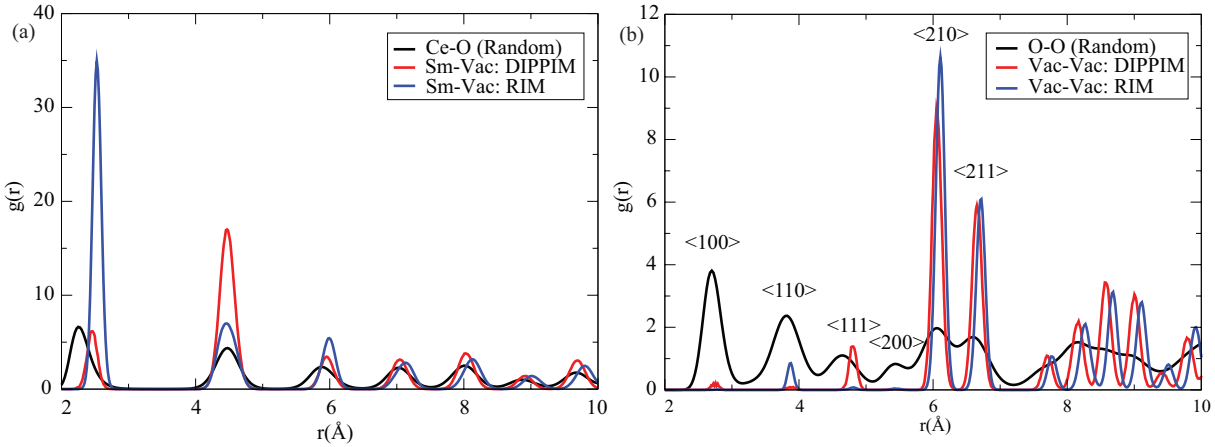

Figure 2. Sm-Vacancy (a) and Vacancy-Vacancy (b) partial radial distribution functions at 973K for $Ce_{0.9}Sm_{0.1}O_{1.95}$, for both the RIM and DIPPIM. The Sm-vacancy RDFs are plotted against the Ce-O RDF representing a randomized distribution of cations and vacancies. The vacancy-vacancy RDFs are plotted against the O-O RDF representing a randomized distribution of vacancies. The labels on peaks in (b) indicate directions in the simple cubic anion sublattice.

4.3. Phonon modes in pure CeO_2

Phonon modes in pure CeO_2 were also investigated as a test for the interatomic potentials. GULP[21] was used for the RIM and a combination of PIMAIM and phonopy[22] for DIPPIM, as DIPPIM is not implemented in GULP. The non-analytical correction (NAC) term, at the Γ-point[23, 24, 25], was included for the DIPPIM in order to determine the splitting between the transverse optical (TO) and longitudinal optical (LO) modes; this was not necessary for the RIM as GULP takes this correction into account. The Born effective charges, Z^*, were taken from Buckeridge *et al.*, with Z^* Ce = 5.525 and Z^* O = 2.764 (obtained using GGA+U)[26] and the high-frequency dielectric constant ($\epsilon^{\infty} = 5.31$) was taken from experiment[27]. This method was found by Buckeridge *et al* to obtain the values most comparable to experiment.

The calculated phonon mode frequencies are displayed in Table 2 for high symmetry points

of the Brillouin zone, Γ, X and L; by definition the RIM will not correctly describe the LO-TO splitting as $\epsilon^{\infty} = 1$, so it is not surprising that the F_{1u} (LO) mode is overestimated by ∼57%. It is of more interest to look at points away from Γ due to this failure to represent LO-TO splitting; the RIM tends to overestimate the phonon modes consistently and on average deviates more from experimental phonon modes when compared with the DIPPIM. This suggests that the RIM is failing to correctly reproduce the motions of the Ce and O ions in the system. This poor estimation of the frequencies by the RIM may lead to less attempted hopping in the system which could account for the poor calculation of ionic conductivity by this model.

Table 2. Calculated phonon mode frequencies of pure CeO_2 at high symmetry points of the Brillouin zone, Γ, X and L, for both the RIM and DIPPIM compared to experiment. Only modes which had available experimental comparisons are presented here. Units of frequency are cm^{-1}.

Mode	RIM	DIPPIM	Expt.
		Γ	
F_{1u} (TO)	291	274	218[28],274[29],275[28]
F_{2g}	524	490	460[29],465[30, 28]
F_{1u} (LO)	920	586	585[28],597[31]
		X	
E_u	187	123	138[29]
E_g	332	211	249[29]
E_u	635	503	464 [29]
		L	
E_u	142	107	138[29]
A_{1u}	256	217	227[29]

5. Conclusions

In conclusion, we have tested two interatomic potentials derived from the same set of ab initio data where one includes polarization effects and the other does not. We have seen that while both potentials reproduce experimental activation energies of oxide ion diffusion, the same can not be said for the ionic conductivity and dopant-vacancy interactions in Sm-doped CeO_2 or the phonon modes in pure CeO_2. Despite the fact that it is ∼10 times more computationally expensive it is necessary to employ the DIPPIM in order to accurately model these materials for SOFC electrolyte applications, due to the large polarizability of the oxide ions.

Acknowledgments

This research was supported by Science Foundation Ireland (SFI) through the Investigators Programme (Grant No. 12/IA/1414). All calculations were performed using the Kelvin (funded through grants from the Higher Education Authority, through its PRTLI program), Lonsdale (funded through a grant from SFI - 06/IN.1/I92/EC07) and Pople (funded by SFI - 12/IA/1414) supercomputers maintained by the Trinity Centre for High Performance Computing (TCHPC), and the Fionn supercomputer, maintained by ICHEC (tcche051b).

References

[1] Williams N R, Molinari M, Parker S C and Storr M T 2015 *J. Nucl. Mater.* **458** 45–55
[2] Yoshiya M and Oyama T 2011 *J. Mater. Sci.* **46** 4176–4190
[3] González-Romero R L, Meléndez J J, Gómez-Garcia D, Cumbrera F L and Dominguez-Rodriguez A 2012 *Solid State Ionics* **219** 1–10
[4] Lewis G V and Catlow C R a 1985 *J. Phys. C Solid State Phys.* **18** 1149–1161

[5] Daw M S and Baskes M I 1984 *Phys. Rev. B* **29** 6443–6453
[6] Rushton M J D and Chroneos A 2014 *Sci. Rep.* **4** 6068
[7] Castiglione M J, Wilson M and Madden P a 1999 *J. Phys. Condens. Matter* **11** 9009–9024
[8] Stambouli A and Traversa E 2002 *Renewanable Sustainable Energy Rev.* **6** 433–455
[9] Kilner J A and Brook R J 1982 *Solid State Ionics* **6** 237–252
[10] Inaba H 1996 *Solid State Ionics* **83** 1–16
[11] Zha S, Xia C and Meng G 2003 *J. Power Sources* **115** 44–48
[12] Burbano M, Nadin S, Marrocchelli D, Salanne M and Watson G W 2014 *Phys. Chem. Chem. Phys.* **16** 8320–8331
[13] Madden P A and Wilson M 1996 *Chem. Soc. Rev.* **25** 339–350
[14] Martyna G J, Tobias D J and Klein M L 1994 *J. Chem. Phys.* **101** 4177–4189
[15] Jung G B, Huang T J and Chang C L 2002 *J. Solid State Electrochem.* **6** 225–230
[16] Omar S, Wachsman E D, Jones J L and Nino J C 2009 *J. Am. Ceram. Soc.* **92** 2674–2681
[17] Kasse R M and Nino J C 2013 *J. Alloys Compd.* **575** 399–402
[18] Marrocchelli D, Madden P A, Norberg S T and Hull S 2011 *Chem. Mater.* **23** 1365–1373
[19] Burbano M, Norberg S T, Hull S, Eriksson S G, Marrocchelli D, Madden P A and Watson G W 2012 *Chem. Mater.* **24** 222–229
[20] Hull S, Norberg S, Ahmed I, Eriksson S, Marrocchelli D and Madden P 2009 *J. Solid State Chem.* **182** 2815–2821
[21] Gale J D and Rohl a L 2003 *Mol. Simul.* **29** 291–341
[22] Togo A and Tanaka I 2015 *Scr. Mater.* **108** 1–5
[23] Pick R, Cohen M and Martin R 1970 *Phys. Rev. B* **1** 910–920
[24] Giannozzi P, De Gironcoli S, Pavone P and Baroni S 1991 *Phys. Rev. B* **43** 7231–7242
[25] Gonze X and Lee C 1997 *Phys. Rev. B* **55** 10355–10368
[26] Buckeridge J, Scanlon D O, Walsh A, Catlow C R A and Sokol A A 2013 *Phys. Rev. B* **87** 214304
[27] Mochizuki S 1982 *Phys. Status Solidi* **114** 189–199
[28] Kourouklis G A, Jayaraman A and Espinosa G P 1988 *Phys. Rev. B* **37** 4250–4253
[29] Clausen K, Hayes W, Macdonald J E, Osborn R, Schnabel P G, Hutchings M T and Magerl A 1987 *J. Chem. Soc. Faraday Trans. 2* **83** 1109–1112
[30] Nakajima A, Yoshihara A and Ishigame M 1994 *Phys. Rev. B* **50** 13297–13307
[31] Marabelli F and Wachter P 1987 *Phys. Rev. B* **36** 1238–1243